Air-induced inverse Chladni patterns: Supplementary Material on the Numerical Method

Henk Jan van Gerner, Ko van der Weele,
Martin A. van der Hoef, and Devaraj van der Meer

In this Supplementary Material, we briefly discuss the hybrid granular dynamics (GD)-computational fluid dynamics (CFD) code that is used in the numerical simulations. The GD code calculates the trajectories of the spherical particles from Newton's law, with the particle-particle interactions being given by a 3D soft sphere collision model including tangential friction. The CFD code calculates the gas phase by evaluating the full Navier-Stokes equations by a finite difference method. The interaction of the gas with the resonating plate is modeled by the immersed boundary method. We next describe each of these elements in more detail.

Particle phase The linear motion of a single spherical particle a with mass m_a and coordinate $\mathbf{r}_a$ is governed by Newton's equations:

$$m_a \frac{\mathrm{d}^2\mathbf{r}_a}{\mathrm{d}t^2} = \mathbf{F}_{\mathrm{grav},a} + \mathbf{F}_{\mathrm{contact},a} + \mathbf{F}_{\mathrm{plate},a} + \mathbf{F}_{\mathrm{drag},a} \,, \tag{1}$$

where $\mathbf{F}_{\mathrm{grav},a} = m_a\mathbf{g}$ is the gravitational force, $\mathbf{F}_{\mathrm{contact},a}$ is the sum of the individual contact forces exerted by all other particles in contact with the particle a, and $\mathbf{F}_{\mathrm{plate},a}$ represents the collision of particle a with the resonating plate. The contact force is divided into a normal and a tangential component:

$$\mathbf{F}_{\mathrm{contact},a} = \sum_{b\in\mathrm{contactlist}} (\mathbf{F}_{n,ab} + \mathbf{F}_{t,ab}) \,. \tag{2}$$

For the calculation of $\mathbf{F}_{n,ab}$ and $\mathbf{F}_{t,ab}$, we use a 3D linear spring/dashpot type of soft sphere collision model [2] along the lines of Cundall and Strack [1]. The particle-plate collisions are modeled in the same way as the particle-particle interactions. Finally, in Eq. (1), $\mathbf{F}_{\mathrm{gas},a}$ represent the gas-particle interaction force (or drag force). In this work, we have chosen simple Stokes drag.
The angular velocity $\boldsymbol{\omega}_a$ of particle a is calculated from:

$$I_a \frac{\mathrm{d}\boldsymbol{\omega}_a}{\mathrm{d}t} = \mathbf{T}_a \,,$$

where $I_a = \frac{2}{5}m_a R_a^2$ is the moment of inertia (with R_a the radius of particle a), and $\mathbf{T}_a$ the torque, which depends only on the tangential component of the individual contact forces:

$$\mathbf{T}_a = \sum_{b\in\mathrm{contactlist}} (R_a\mathbf{n}_{ab} \times \mathbf{F}_{t,ab}) \,,$$

where $\mathbf{n}_{ab}$ is the normal unit vector from particle a to b.

Gas Phase The gas flow is governed by the conservation equations for mass and momentum:

$$\frac{\partial(\rho_g)}{\partial t} + \nabla\cdot\rho_g\mathbf{u} = 0 \,, \tag{3}$$

$$\frac{\partial(\rho_g\mathbf{u})}{\partial t} + \nabla\cdot\rho_g\mathbf{u}\mathbf{u} = -\nabla p - \nabla\cdot\boldsymbol{\tau} + \rho_g\mathbf{g} + \mathbf{s}_{\mathrm{ibm}} \,, \tag{4}$$

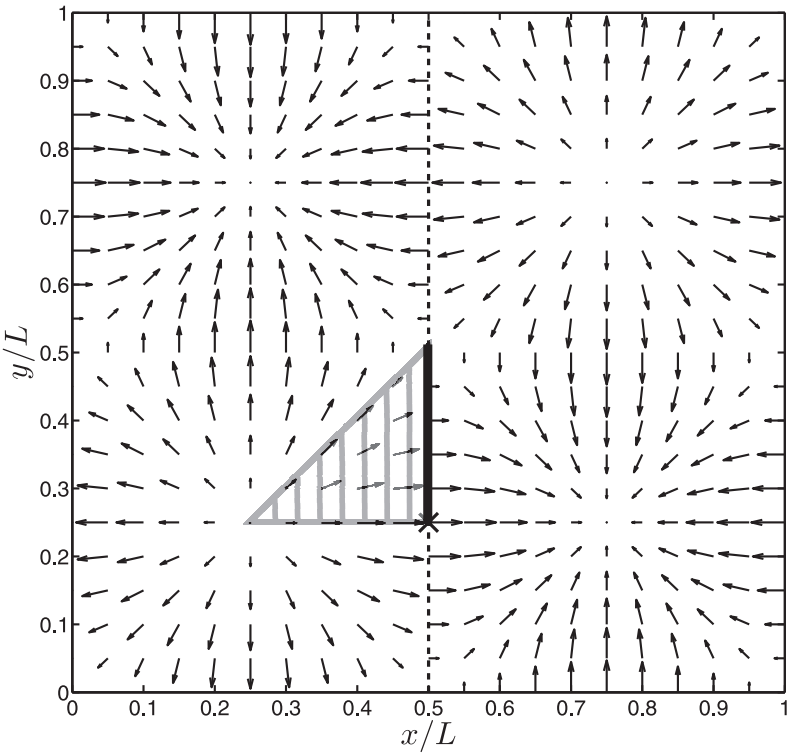

Figure 1: Horizontal flow field at $t = \frac{1}{2}/f$ s over a vertically vibrating flexible bottom plate.

where p is the gas phase pressure, $\boldsymbol{\tau}$ the viscous stress tensor, $\mathbf{s}_{\mathrm{ibm}}$ the source term for the momentum exchange with the plate. The pressure and gas-phase density are linked by the ideal gas law. In principle Eq. (4) should also contain the force density arising from the interaction with the solid particles. However, as explained in the main text, for computational reasons we have not considered the influence of the particles on the flow field, which is expected to be very small in any case. In order to numerically solve eqs. (3)- (4), a first-order-accurate semi-implicit method is used to discretize the momentum equations in time. The pressure and the particle force contribution are treated implicitly, while the viscosity and convection contribution are treated explicitly. A staggered Cartesian 3D grid (cell size δl) is used for the spatial discretization. The scalar variables (p and ρ_g) are defined at the cell center, whereas the velocity components are defined at the cell faces. The convective fluxes are computed using a second-order flux delimited Barton scheme [3, 4], where the viscous and pressure terms are calculated by a central difference representation. The resulting set of equations are solved iteratively, by the SIMPLE algorithm, where the pressure is adapted via a Newton-Rhapson procedure until mass conservation is achieved. Details of the procedure can be found elsewhere [2].

Gas-plate interaction In previous studies we have used a simplified method to model gas flow in vibrated beds [7], where the vibrating bottom moves through the computational cell, so that it cuts the cell, which has to be taking into account in the computional procedure. In the present paper, we have used a more sophisticated and flexible approach, where the interaction of the gas phase with the resonating plate is modeled with the immersed boundary (IB) method. In this method, the resonating surface is "bespeckled"

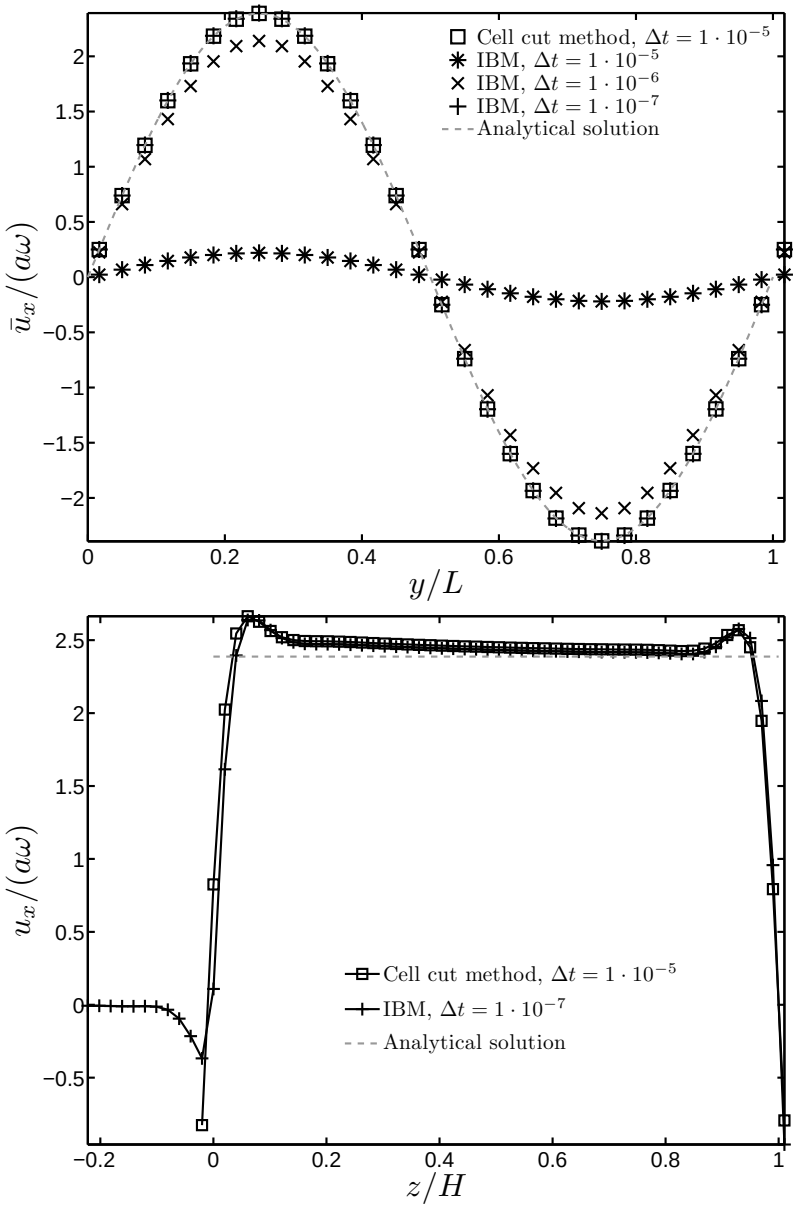

Figure 2: (top) Analytical and simulated velocity $\bar{u}_x$ at $x = L/2$ (dashed line in Fig. 1). (bottom) Simulated velocity u_x at $x = L/2$ and $y = L/4$ (indicated by the black X in Fig. 1). For both numerical methods, the no slip condition is used at the top and bottom boundary, resulting in a thin boundary layer. With the immersed boundary (IB) method, the flow field is also calculated underneath the vibrating bottom plate, indicated by the plus markers located at $z < 0$.

with markerpoints, with a surface density of the order of a few points per δl^2, where δl is the grid size of the CFD model. Each of these marker points exerts a force on the fluid, and the corresponding force density is included in the hydrodynamics equations of the gas-phase, and thus also included the CFD scheme. The magnitude of this force can be tuned such that the gas-phase velocity vanishes at the location of the marker point, thereby modeling "no-slip" boundary conditions. The IB method has been widely used to study fluid-structure interaction and was pioneered by Peskin [5] to investigate cardiac flow problems. Subsequently, the method has been extended to the flow around rigid bodies. The implementation that we adopt is along the lines of Uhlmann [6], where we have also included an extra iteration loop to improve the match between the actual and desired velocity at the location of the plate.

In order to validate the implementation, we have simulated a container with dimensions $150 \times 150 \times 5$ mm^3 which is divided in $30 \times 30 \times 50$ CFD cells ($L \times L \times H$). For the top of the container, a no-slip boundary is used while periodic boundaries are used for all the vertical walls. The vertical position z of the bottom plate at any point (x, y) is given by:

$$z(x, y, t) = a \sin(\omega t) \sin \frac{2\pi x}{L} \sin \frac{2\pi y}{L} \ , \tag{5}$$

with $\omega = 2\pi f = 2\pi$ 200 rad/s and $a = 2.5 \cdot 10^{-5}$ m (corresponding to a dimensionless acceleration $\Gamma = 4$). The horizontal velocity of the gas, averaged over the height H, can be evaluated analytically and is equal to (see Fig. 1):

$$\bar{u}_x = R\, a\omega \cos(\omega t) \cos \frac{2\pi x}{L} \sin \frac{2\pi y}{L}, \tag{6}$$

$$\bar{u}_y = R\, a\omega \cos(\omega t) \sin \frac{2\pi x}{L} \cos \frac{2\pi y}{L} \ , \tag{7}$$

where the amplitude R has yet to be determined. This amplitude can be derived with a continuum and symmetry consideration: All the air that is displaced vertically by the resonating plate within the hatched area in Fig. 1, must flow horizontally through the area indicated by the thick black line, which results in $R = L/(4\pi H)$. Figure 2 (top) shows the analytical and simulated velocity $\bar{u}_x$ at $x = L/2$ (dashed line in Fig. 1). For the cell cut method, the agreement with the analytical solution is excellent. For the immersed boundary method, the agreement using a Δt of $1 \cdot 10^{-5}$ s is very poor. Decreasing the time step to $1 \cdot 10^{-7}$ s greatly improves the agreement. However, a similar agreement can also be obtained by using a Δt of $1 \cdot 10^{-6}$ s and 4 IBM iterations or a Δt of $1 \cdot 10^{-5}$ s and 25 IBM iterations (not shown in Fig. 2). Note that for the simulations described in this paper, we have chosen a much finer grid; it was found that a timestep of $2 \cdot 10^{-5}$ s with 10 iterations gave sufficiently accurate results.

The simulated velocity u_x as a function of z at $x = L/2$ and $y = L/4$ (black X in Fig. 1) is shown in Fig. 2 (bottom). Again we find that the cell-cut method and the IB method give comparable results, provided that the timestep is sufficiently small.

References

[1] P.A. Cundall, O.D.L. Strack, *A discrete numerical model for granular assemblies*, Géotechnique **29**, p. 47 (1979).

[2] M.A. van der Hoef, M. Ye, M. van Sint Annaland, A.T. Andrews IV, S. Sundaresan, J.A.M. Kuipers, *Multi-scale modeling of gas-fluidized beds*, Adv. Chem. Eng. **31**, p. 65 (2006).

[3] J. Centrella, J.R. Wilson, *Planar numerical cosmology. II. The difference equations and numerical tests*, Astrophys. J. Suppl. Ser. **54**, 229 (1984).

[4] J.F. Hawley, L.L. Smarr, J.R. Wilson, *A numerical study of nonspherical black hole accretion. II. Finite differencing and code calibration*, Astrophys. J. Suppl. Ser. **55**, 211 (1984).

[5] C.S. Peskin, *The immersed boundary method*, Acta Numerica **11**, p. 480 (2002).

[6] M. Uhlmann, *An immersed boundary method with direct forcing for the simulation of particulate flows*, J. Comp. Phys. **209**, p. 448 (2005).

[7] C. Zeilstra, *Simulation of density segregation in vibrated beds*, Phys. Rev. E **77**, 031309 (2008).